Springer

KSME

Journal of Mechanical Science and Technology 28 (9) (2014) 3433~3442
www.springerlink.com/content/1738-494x
DOI 10.1007/s12206-014-0804-0

A dynamic model of ball bearing for simulating localized defects on outer race using cubic hermite spline †

P. G. Kulkarni[1,*] and A. D. Sahasrabudhe[2]

[1]*Department of Mechanical Engineering, PVG's COET, Pune, 411009, India*
[2]*College of Engineering, University of Pune, Pune, 411005, India*

(Manuscript Received January 13, 2014; Revised May 9, 2014; Accepted May 22, 2014)

Abstract

In this paper a dynamic model is presented for predicting the vibration behavior of a ball bearing under the influence of localized defects on the outer race. The calculation of contact force is based on Hertzian contact deformation theory. The pulse generated by the ball striking the defect on outer race is modeled by using the blending functions of the cubic hermite spline. The effect of change in the angular position of the defect, size of the defect on outer race, multiple defects on outer race and the variation of load on the vibration amplitude is predicted by this model. A computer program in MATLAB is developed and the governing equation of motion is solved by Euler's method. The numerical results are presented as a function of variation of the geometry of the outer race due to the impact at the defect and normal race contact w.r.t. time and the conclusion about the health of the bearing is determined by the spectral analysis. To validate the results, experimentation has also been performed.

Keywords: Ball bearing; Cubic hermite spline; Spectral analysis; Vibration

1. Introduction

Rolling element bearings are among the most important and critical components in mechanical systems. A damaged bearing in a machine acts as a vibration generator and has a great impact on the performance of the entire system. This outlines the need for monitoring the health of bearing from time to time to avoid sudden failure of the system. The damage in a bearing is due to different defects present on races and rolling elements. The manufacturing process itself may give rise to these defects or these may develop during the service conditions. Different measurement techniques based on vibration and acoustics are used for detecting the defects in a bearing. In addition to the experimental methods, the analytical methods are also used by the researchers which yield reasonably accurate results to predict the dynamic behavior of bearing.

A geometrically perfect bearing is a source of vibration since the load is carried by finite number of balls. As bearing rotates, the position of the balls in the load zone changes giving rise to periodical variation of total stiffness of bearing assembly. Sunnersjo [1] has carried out the study on the effect of varying compliance on vibrations of rolling bearings. But the vibration level of bearing is significantly altered in the presence of defects. A detailed description of these defects are available in standard books on bearings [2, 3]. Tandon and Choudhury [4] presented a detailed review of vibration and acoustic measurement methods for detection of defects in rolling element bearings and considered localized and distributed defects. When a defect strikes its mating surface, a pulse of short duration is generated as a result of sudden change in the contact stress. It is the frequency of pulse generation which is to be monitored and describes the location of fault. Harris [2] explained the fundamental kinematic analysis for modeling the performance of rolling element bearings. McFadden and Smith [5, 6] have presented a model which describes the modulating influences on impulses generated by single point and multipoint defects on the inner race of bearings. Su and Lin [7] extended the vibration model developed by McFadden and Smith to describe the bearing vibration under diverse loading. They have reported the need of time domain analysis along with frequency domain to reliably monitor a running bearing. Tandon and Choudhury [8] proposed an analytical model for predicting the vibration frequencies of rolling bearings and the amplitudes of significant frequency components due to a localized defect on outer race, inner race or one of the rolling elements under the axial and radial loads. The model considers the effect of load and pulse shape on the vibration amplitude. Sawalhi and Randall [9] presented a combined gear/bearing dynamic model for a gearbox test rig to study the

*Corresponding author. Tel.: +91 9890265462, Fax.: +91 2024226858
E-mail address: prof.pgk@gmail.com
† Recommended by Associate Editor Cheolung Cheong

interaction between gears and bearings in the presence of faults. Patel et al. [10] presented a dynamic model to study the vibrations of deep groove ball bearings having single and multiple defects on surfaces of inner and outer races. The authors have considered masses of shaft, housing, races, and balls in the model. The additional deflection due to the interaction of the ball at the defect was defined in terms of the width of the defect. Patil et al. [11] have presented an analytical model for predicting the effect of a localized defect on the ball bearing vibrations. The contacts between the ball and the races were considered as non-linear springs. The pulse generated by striking of the defect was modeled as half sine wave. Harsha et al. [12] developed an analytical model to predict non-linear dynamic response in a rotor bearing system due to surface waviness. In the analytical formulation, the contacts between the rolling elements and the races were considered as non-linear springs, whose stiffness is obtained by using Hertzian elastic contact deformation theory. Purohit and Purohit [13] presented an analytical model of a rotor bearing system to observe the effect of varying the number of balls and preload on the vibration characteristics of a defect free system. They concluded that for larger preloads, the vibration amplitudes associated with the ball passage frequency reduces and increasing the number balls results in reduction in the vibration amplitude.

Based on the literature survey, it is found that the pulse generated by impact at the defect is modeled as a half sine wave, triangular and rectangular wave. However, for modeling of the defect pulse, splines may prove equally good. It is found that there are no investigations on the use of splines in such study. With the rotation of the cage, the ball will alter the geometry of the outer race. As the defect on the outer race on the bearing gets struck by the rolling elements, the geometry of the movement of the races changes and a pulse of very short duration is generated. The action of the ball orbiting the inner race is analogous to the cam with the outer race acting as a follower. This phenomenon forms the basis for using blending functions of the cubic hermite spline for modeling the pulse generated by the striking of the defect. Essentially the shape of the pulse is assumed according to the physical phenomenon happening inside the bearing which is discussed in detail in the next section.

2. Formulation of the mathematical model of system

At the end of the shaft of rotor-bearing system being analyzed, a deep groove ball bearing (designation: SKF 6205) is mounted as a test bearing as shown in Fig. 1. The inner race of the bearing is rigidly fixed to the shaft and the outer race is fixed in a rigid support. The elastic deformation between the outer race and each point of contact with the balls is assumed be Hertzian. In the mathematical model, the ball bearing is considered as non-linear spring-mass system. The model presented here considers the specific case of a non-rotating outer race, loaded radially.

Fig. 1. Rotor-bearing system.

The assumptions and considerations while deriving the model are summarized as follows:

- The ball bearing model has equi-spaced balls rolling on the surface of the inner and outer race and there is no interaction between them.
- Slipping of the balls during rolling on races is neglected.
- The motions of race and balls occur in the plane of the bearing only.
- The inner race of the bearing is rigidly fixed to the shaft and the outer race is fixed in a rigid support.
- Deformations at the contacts are Hertzian contact deformations.
- The bearings operate under isothermal conditions.
- The shape of the pulse generated by impact at the defect as shown in Fig. 8 models the defect.

2.1 Internal speeds, motions and load distribution in a ball bearing

Ball bearings are used to support various kinds of loads while permitting rotational motion of a shaft. The expressions for rolling bearing internal rotational speeds are developed by Harris [2]. When a bearing mounted on a shaft rotates at some speed, the rolling elements orbit the bearing axis and simultaneously revolve about their own axes (refer Fig. 2).

The rotational speed of the cage is given by

$$n_c = \frac{1}{2}\left[n_s\left(1-\frac{D}{d_m}\right)\right]. \tag{1}$$

The angular velocity of the cage is

$$\omega_c = \frac{1}{2}\left[\omega_s\left(1-\frac{D}{d_m}\right)\right]. \tag{2}$$

Angular velocity of balls is defined by the following relation:

$$\omega_R = \frac{1}{2}\frac{d_m}{D}n_s\left(1-\frac{D^2}{d_m^2}\right). \tag{3}$$

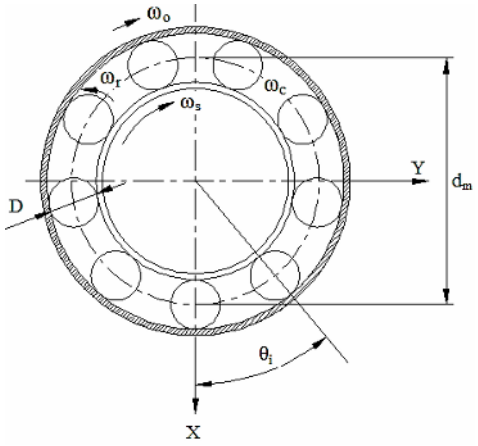

Fig. 2. Rolling speeds and velocities.

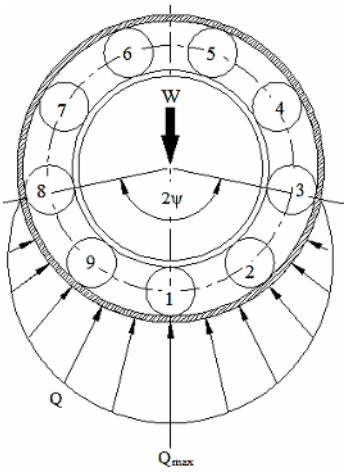

Fig. 3. Bearing load distribution.

Bearing load distribution (refer to Fig. 3) with respect to angular position of ball is calculated by Eq. (4):

$$Q_\theta = Q_{max}\left[1-\frac{1}{2\epsilon}(1-cos\Psi)\right]^{3/2} \quad (4)$$

where $\epsilon = \frac{1}{2}\left(1-\frac{\gamma}{2\delta_{max}}\right)$.

2.2 Calculation of restoring force

In general, the deflection of the ith ball located at any angle θ is calculated by following expression (refer to Fig. 4):

$$\delta = (xcos\theta_i + ysin\theta_i) - (\gamma). \quad (5a)$$

x and y are the deflections along X and Y direction respectively and γ is the internal radial clearance which is the clearance between an imaginary circle, which circumscribes the balls and the outer race. At the time of impact at the defect, a pulse of short duration is produced and it is accounted for by the term Δ i.e. additional deflection. Hence, Eq. (5a) is modified by adding Δ to internal radial clearance and is given by

$$\delta = (xcos\theta_i + ysin\theta_i) - (\gamma + \Delta). \quad (5b)$$

The restoring force generated by ball-race contact deformation of the ball is of nonlinear nature because of the Hertzian contact. The local Hertzian contact force and deflection relationship for bearing may be written as

$$F_{\theta_i} = K(\delta)^n, n = 3/2 \quad (6a)$$

where K is the constant for Hertzian contact elastic deformation which depends on the contact geometry.

Substituting δ from Eq. (5b) in Eq. (6a), we get

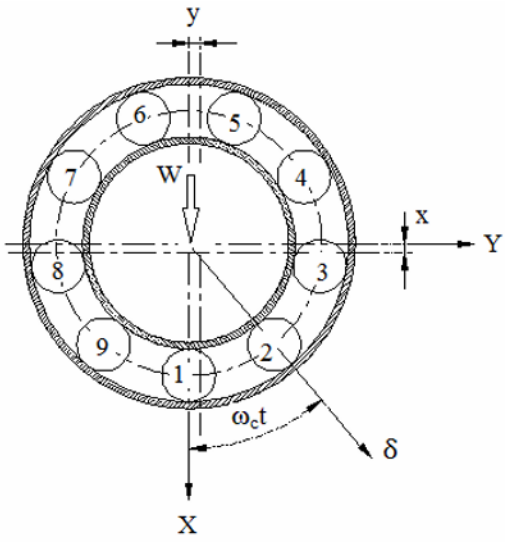

Fig. 4. Schematic diagram of a rolling element bearing.

$$F_{\theta_i} = K[(xcos\theta_i + ysin\theta_i) - (\gamma + \Delta)]^{3/2}. \quad (6b)$$

For the contact of each ball in non-defective region, referred to as normal race contact, additional deflection, Δ is zero. The restoring force is resolved along directions X and Y. The components of the restoring force are

$$F_X = \sum_{i=1}^{Z} K[(xcos\theta_i + ysin\theta_i) - (\gamma + \Delta)]^{3/2} cos\theta_i \quad (6c)$$

$$F_Y = \sum_{i=1}^{Z} K[(xcos\theta_i + ysin\theta_i) - (\gamma + \Delta)]^{3/2} sin\theta_i \quad (6d)$$

where z = No. of balls.

Fig. 5 shows the contact between mating surfaces of revolution. Under no load condition, point contact exists between the

Table 1. Input data for the model.

Inner race diameter	31.1 mm
Outer race diameter	46.98 mm
Pitch diameter	39.04 mm
Ball diameter	7.94 mm
Internal radial clearance	20 μm
Radial load	424 N
Mass of rotor	4 kg
No of balls	9
Speed of rotor	2400 rpm
Damping factor	200 Ns/m
Contact angle	0^0

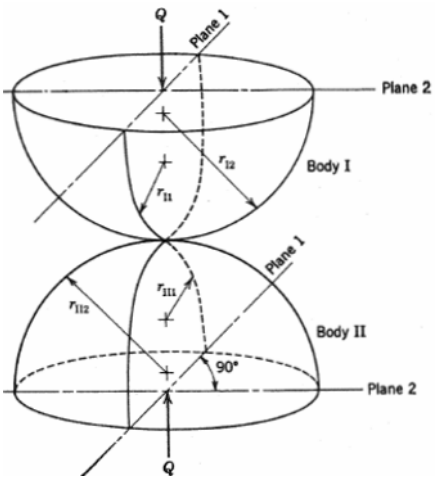

Fig. 5. Geometry of contacting bodies.

ball and race which changes to area contact which has the shape of an ellipse. The two terms curvature sum and curvature difference describe the contact between the mating surfaces. Curvature sum ∑ρ is calculated using the radii of curvature in a pair of principal planes passing through the point contact and using curvature difference F(ρ), dimensionless contact deformation δ^* is calculated [2]. The effective elastic modulus K for the bearing system is written as:

$$K = \left[\frac{1}{\left(1/K_i\right)^{1/n} + \left(1/K_o\right)^{1/n}}\right]^n . \tag{7a}$$

The elastic modulus for the contact of a ball with the inner race is

$$K_i = 3.587 \times 10^7 (\sum \rho_i)^{-1/2} (\delta_i^*)^{-3/2} \quad \left(\frac{\mathrm{N}}{\mathrm{mm}^{3/2}}\right). \tag{7b}$$

Similarly, the elastic modulus for the contact of a ball with the outer race is

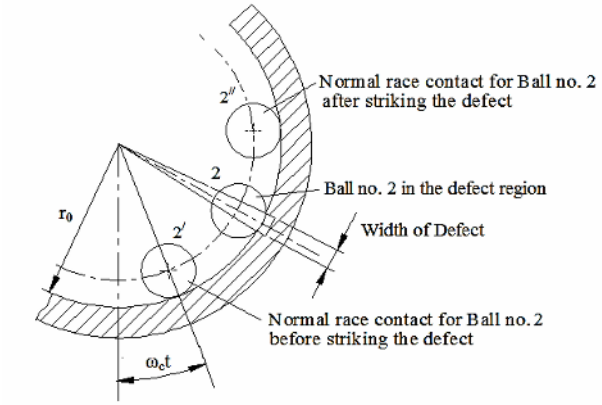

Fig. 6. Different positions of ball no. 2 relative to the outer race defect.

$$K_0 = 3.587 \times 10^7 (\sum \rho_0)^{-1/2} (\delta_0^*)^{-3/2} \quad \left(\frac{\mathrm{N}}{\mathrm{mm}^{3/2}}\right). \tag{7c}$$

The value of K for 6205 bearing is 49582 N/mm [14].

2.3 Simulation of local defects using blending functions of cubic hermite spline

This section describes mathematical simulation of localized defects on outer race. Cracks, pits, spalls are included in the class of localized defects. When such a defect on one surface strikes its mating surface, a pulse of short duration is produced. This pulse represents the severity, extent and age of the damage. These factors have influence on the amplitude of response. Different pulse forms being used for this situation are rectangular, triangular, half-sine pulse etc. This pulse being of short duration, there is tendency to neglect the pulse width. In real situation, the pulse generated due to impact at the defect may not be of such a regular shape. Rectangular, triangular forms are the approximations for the shape of the real pulse and are the two extremities (non-realistic) in between which the shape of the defect pulse lies in actual situation. Half sine pulse is one of the cases lying in between these two extreme forms. For the pulses of regular shape, the variation in displacement is gradual throughout which may not happen in real situations depending on the form of defect. Secondly, this assumption is based on the fact that displacement at all intermediate points between the two instances; entry of ball in the defect region and exit at the defect are known. In real situation, displacement at intermediate points are dictated by the shape of the defect, depth of the defect and width of the defect, based on which the real pulse will assume some shape.

In the present study, the simulation of the defect pulse using cubic Hermite spline is based on the assumption that the displacements at intermediate points are difficult to predict and the more realistic assumption would be to assume displacement behaviour at the entry edge of the defect and exit edge of the defect. In case of cubic Hermite spline, displacements at the control points (intermediate points) are not known. Instead

displacements at the start and end points are known. At the starting edge of the defect, ball retards due to loss of contact with the outer race and at this instant the displacement is assumed to be -1 as shown in Fig. 8. As the ball leaves the defect, it accelerates due to regaining of contact with the outer race and the displacement is assumed to be +1. Hence, the displacement law is retardation followed by acceleration. As opposed to this, in case of regular shapes, the displacements are gradual which is far from reality.

As every ball establishes and breaks the contact with the defective region of the outer race shown in Fig. 6, the geometry of race movement will change. The behavior of ball establishing and breaking the contact with the race is similar to cam (follower) jump phenomenon. Essentially the ball orbiting the inner race acts as a cam and the outer race acts as the follower. For normal race contact, there is hardly any change in the geometry of the movement. During the travel of the ball in the defective region of the outer race, the locus of race center position as a function of angle θ and its time derivatives are to be obtained through the mathematical modeling of the system. While developing the computer program, it is ensured that the ball at θ is the only one in the defective region. The ball ahead of it (leading) has lost its contact with the defective region and the ball lagging behind is waiting for its contact with the defective region.

In mathematics, a spline is a sufficiently smooth polynomial function that is piecewise defined and it possesses a high degree of smoothness at the places where the polynomial pieces connect. Splines are curves which are usually required to be continuous and smooth. Cubic spline interpolation is a fast, efficient and stable method of function interpolation between key points. In spline interpolation, the interpolation interval is divided into small subintervals. Each of these subintervals is interpolated by using the third-degree polynomial. The polynomial coefficients are chosen to satisfy certain conditions. General requirements are function continuity passing through all given points and continuity of higher derivatives etc. In hermite interpolation, the function value and the value of the first derivative are known at each interpolating point. Interpolation with derivative values is also known as osculatory interpolation. Hermite curves are very easy to calculate but also very powerful. To calculate a hermite curve, the following vectors are needed:

1. P_0 = the start point of the curve.
2. P_0' = the tangent at the start point describing how the curve leaves point P_0.
3. P_1 = the endpoint of the curve.
4. P_1' = the tangent at the endpoint of the curve.

These four vectors are simply multiplied with four hermite basis functions shown in Fig. 7 and added together. These blending functions are given by Eqs. (8a)-(d):

$$H_0(t) = 2t^3-3t^2+1 \quad (8a)$$
$$H_1(t) = -2t^3+3t^2 \quad (8b)$$
$$H_2(t) = t^3-2t^2+t \quad (8c)$$

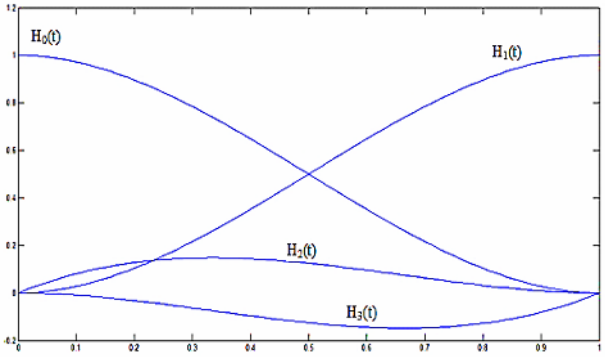

Fig. 7. Hermite blending functions.

$$H_3(t) = t^3-t^2. \quad (8d)$$

The function $H_0(t)$ starts at 1 goes slowly to 0. Function $H_1(t)$ starts at 0 and goes slowly to 1. Multiply the start point with $H_0(t)$ and the endpoint with $H_1(t)$. Let t go from 0 to 1 to interpolate between known start and end points. $H_2(t)$ and $H_3(t)$ are applied to the tangents in the same manner. They make sure that the curve blends in the desired direction at the start and end point. Blending functions point wise can be written as

$$P(t) = (2t^3-3t^2+1)P_0+(-2t^3+3t^2)P_1+(t^3-2t^2+t)P_0'+(t^3-t^2)P_1' \quad (9a)$$
$$P'(t) = (6t^2-6t)P_0+(-6t^2+6t)P_1+(3t^2-4t+1)P_0'+(3t^2-2t)P_1'. \quad (9b)$$

Substituting $P_0 = -1$ and $P_1 = 1$ in Eq. (9a), equation of the curve is written as

$$S = -4t^3+6t^2-1. \quad (9c)$$

For 1mm defect size on outer race 't' in MATLAB program is calculated as

$$t = 0:0.043478:1 \quad (9d)$$

where time step = 0.043478 = 1/stay instants of ball in outer race defect (23 for 1 mm defect size). The Stay instants of ball in outer race defect changes linearly depending on the defect size. The effect of bearing degradation is simulated in the mathematical model by considering different defect sizes such as 0.5 mm, 1 mm, 1.5 mm. The shape of the pulse remains same but the size varies when there is change in the defect size. This is one of the features of the defect pulse modelled by cubic hermite spline. The simulated pulse generated as a result of impact at the defect is shown in Fig. 8. Normal race contact in Fig. 8 refers to the normal geometrical movement of the outer race i.e. when the defect lies between the neighboring balls and is not getting struck. When the defect gets struck, the movement of the outer race geometry changes resulting in generation of the pulse as described in the previous section.

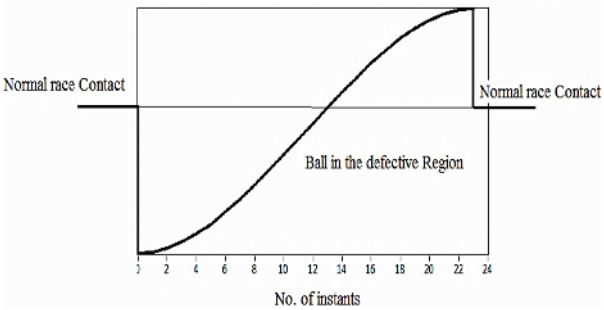

Fig. 8. Simulated Pulse generated by impact at the defect.

2.4 Equation of motion

Taking x and y as the displacements along X and Y directions, the governing equations accounting for inertia, damping and restoring forces and constant vertical force in X direction for a two degree of freedom system are formed.

$$M\ddot{x} + C\dot{x} + \sum_{i=1}^{Z} K[(x\cos\theta_i + y\sin\theta_i) - (\gamma + \Delta)]^{3/2} \cos\theta_i = W \tag{10}$$

$$M\ddot{y} + C\dot{y} + \sum_{i=1}^{Z} K[(x\cos\theta_i + y\sin\theta_i) - (\gamma + \Delta)]^{3/2} \sin\theta_i = 0\,. \tag{11}$$

The system of Eqs. (10) and (11) are two coupled non-linear ordinary second order differential equations. Here Δ term corresponds to additional deflection for the travel of ball in the defective region of the outer race which is modeled by cubic Hermite spline. This Δ term is calculated based on Eqs. 9(c) and (d) and is graphically represented in Fig. 8. For normal race contact, Δ i.e. additional deflection will be zero. The damping in this system is represented by an equivalent viscous damping C.

3. Results and discussion

3.1 Computational procedure

Using Euler's method Eqs. (10) and (11) are solved and the displacements in X and Y directions and their time derivatives are obtained. Initial conditions of x and y are 10^{-6}. The time step of 1.745×10^{-5} sec has been considered in the computation which corresponds to 0.1^0 bearing rotation increment. A computer program in MATLAB is developed for solving the equations.

For a shaft speed N_s = 2400 rpm.
Cage speed, ω_c = 100 rad/sec.
Ball pass frequency of outer race, fod = 144 Hz.

3.2 Effect of change in the angular position of defect on outer race

To study the effect on the amplitude level of vibration with change in position of the defect on outer race, the angular position of the defect is changed in steps at 424 N constant

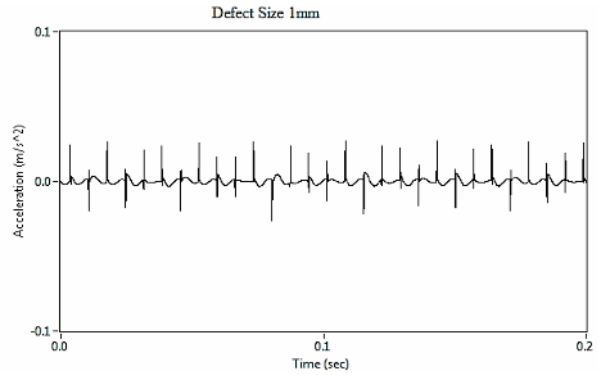

Fig. 9. Time waveform for defect on outer race at 424 N radial load.

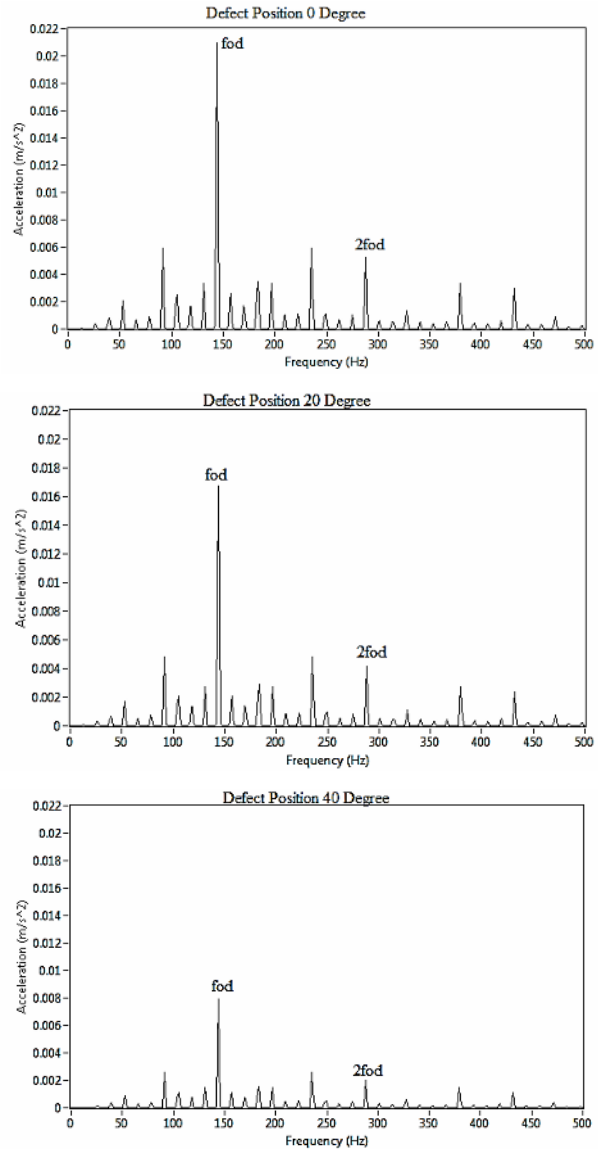

Fig. 10. Frequency spectra for different defect positions at 424 N radial load.

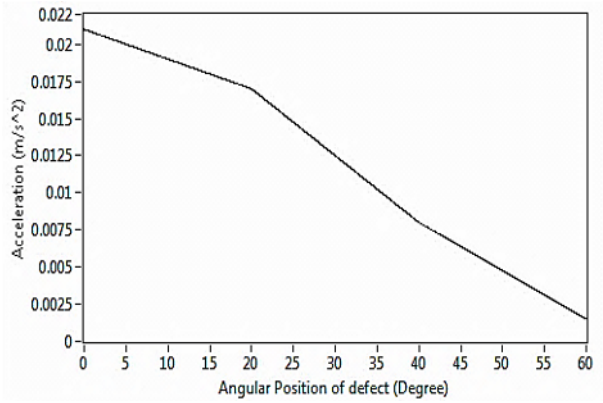

Fig. 11. Variation of amplitude with angular position of defect at 424 N radial load.

radial load. The reference position of the defect is assumed at 0^0 and in this position of the defect, the defect is just below the load and the expected amplitude level is high. Fig. 9 shows the time waveform for 1 mm defect on outer race at 424 N radial load.

Fig. 10 shows the spectra for different angular positions of the defect on outer race.

The theoretical ball pass frequency of outer race (BPFO) is 144 Hz. The spectra for different conditions of loading and position of defect shows dominant peak at this frequency and its second harmonic. When the defect is at 0 degree, i.e. just below the load, the amplitude of vibration is maximum. As the position of the defect is changed away from this reference position, it is observed that the amplitude of vibration reduces. This variation is shown in Fig. 11.

3.3 Effect of variation of radial load with defect size of 0.5 mm, defect at 60 degree on outer race

The radial load on the bearing was varied in steps from 212 N to 848 N. The frequency spectra for different loading are shown in Fig. 12. The variation of amplitude with the radial load is plotted in Fig. 13. It is observed that, for the outer race defect, with the increase in load, there is significant increase in the amplitude level.

3.4 Effect of outer race defect size

To study the effect of defect size, the load is kept constant at 424 N and the time step in Eq. (9d) is varied depending on the size of defect on outer race.

The results of increase in the defect size are shown in Fig. 14. It is observed that the amplitude level increases with the increase in defect size.

3.5 Effect of two defects on outer race

To study the effect of two defects on outer race, additional defect is simulated at 180^0 to the existing defect. This is done

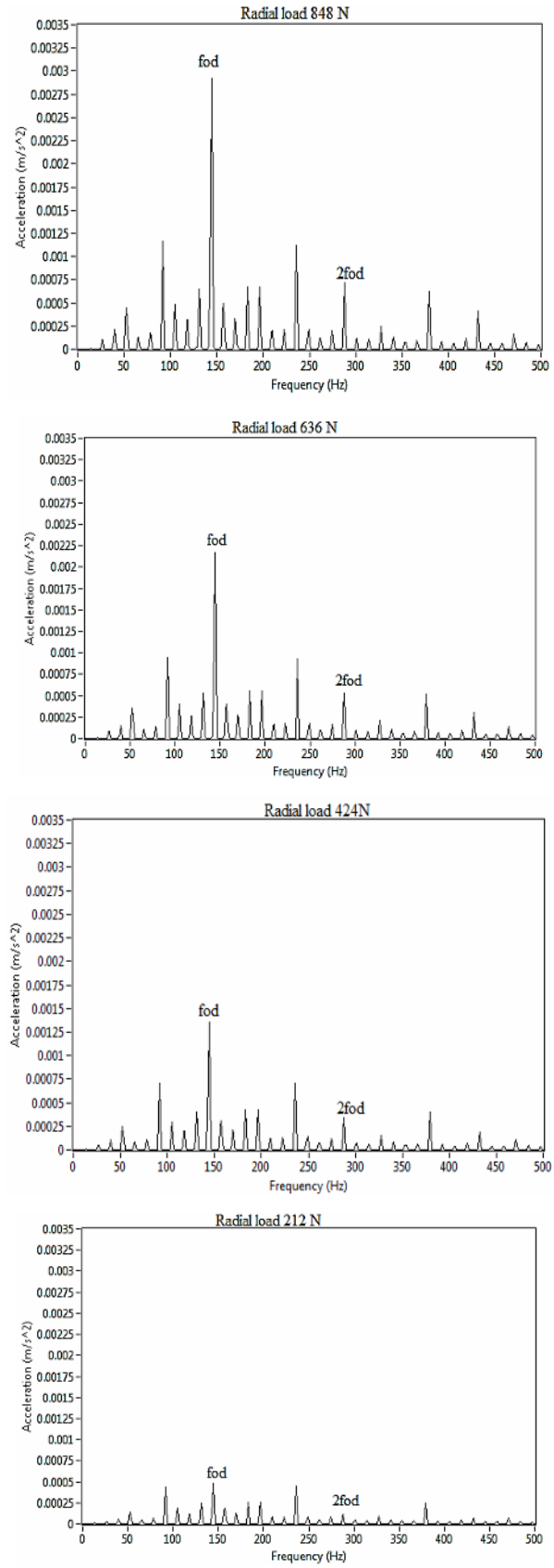

Fig. 12. Frequency spectra for 0.5 mm defect on outer race at 60^0 for different radial loads.

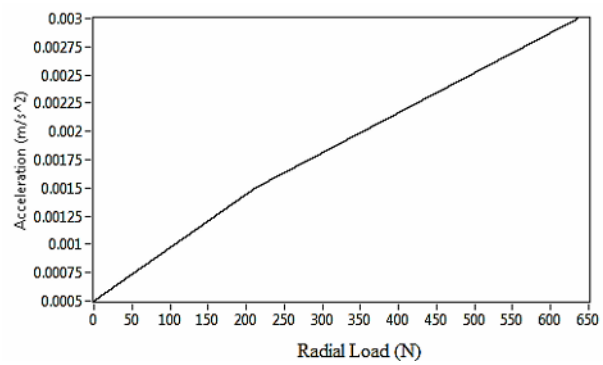

Fig. 13. Variation of amplitude with radial load.

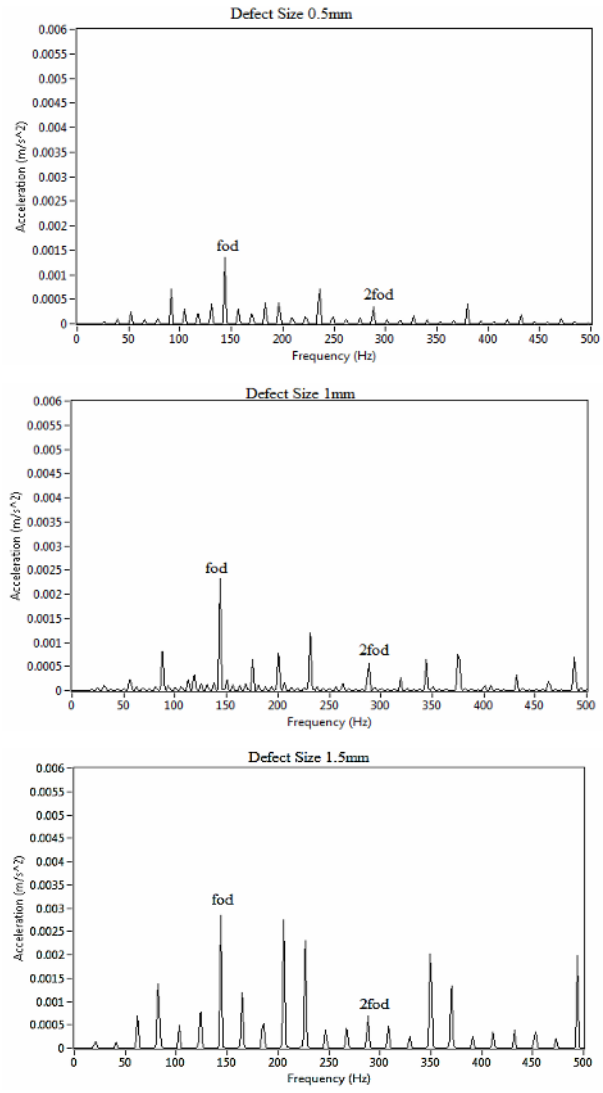

Fig. 14. Effect of outer race defect size.

for 1mm defect size and at 424 N constant load. Based on spectra shown in Fig. 15, it can be concluded that the vibration amplitude is almost doubled in case of two defects 180^0 apart as compared to a single defect on outer race.

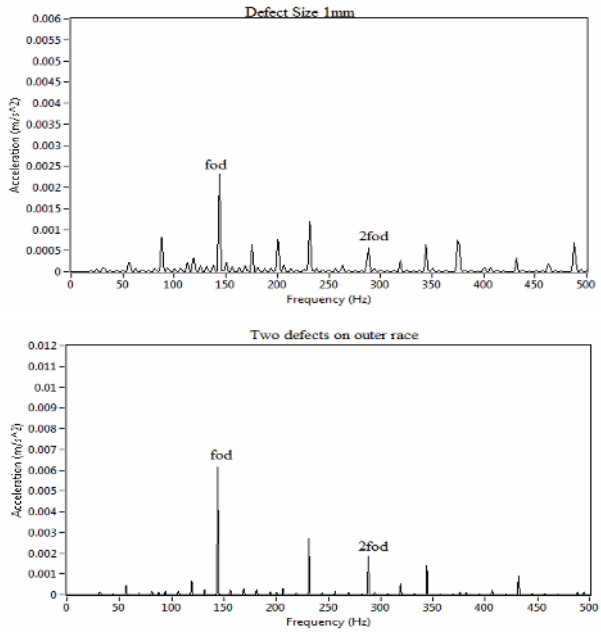

Fig. 15. Effect of two defects on outer race.

Fig. 16. Experimental setup.

4. Experimentation

In the present work, the vibration signatures are collected from the bearing of an experimental set up shown in Fig. 16. The shaft of the experimental setup is driven by an AC motor equipped with a variable frequency drive. The test bearing, a single-row deep groove ball bearing (SKF 6205) is placed in the bearing housing at the non-drive end of the shaft and loaded by screw and nut arrangement in radial direction. The vibrations of the bearing are recorded using PCB shear accelerometer with a sensitivity of 100 mv/g. The accelerometer mounted on the test bearing housing is connected to NI 9234 sound and vibration card. Using this hardware, the time domain signals of the test bearings are acquired and processed in Lab VIEW software. The defects were created on the outer race by electric discharge machining. The signals are sampled at 10 kHz with 4096 samples. For the experimentation, bearing was run at 2400 rpm.

Figs. 17 and 18 show the experimental results of the defective bearing with the defect on outer race. There is slight

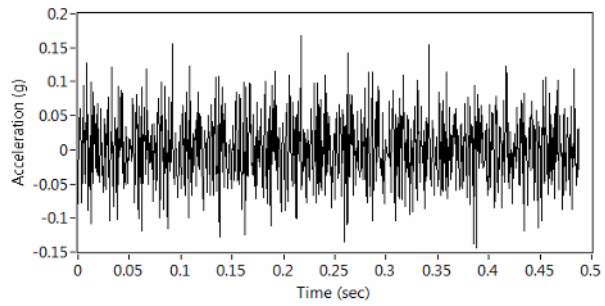

Fig. 17. Time waveform of defective bearing at 2400 rpm (experimental).

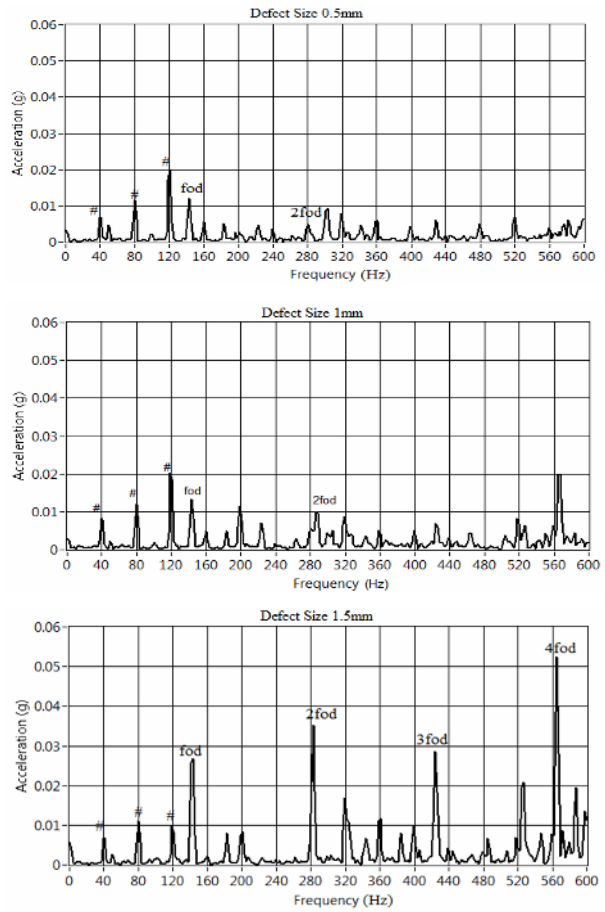

Fig. 18. Effect of outer race defect size at 2400 rpm (experimental).

variation of about 4% in the theoretical and experimental values of outer race defect frequency. The amplitude of vibration predicted by the model and obtained through experimentation differs because of the fact that the theoretical model does not account for contribution of each element in the vibration of rotor bearing system. It is observed that with the increase in defect size on outer race, the amplitude of vibration increases as predicted by the theoretical model.

5. Conclusions

(1) In the present study a theoretical model is developed to predict the vibration produced by bearing with the defect on outer race. The model simulates the effect of radial load, effect of defect size, its position and effect of multiple defects and predicts the presence of fault on the outer race of bearing by showing peak in the spectrum at the characteristic defect frequency. The frequency spectrum obtained from mathematical model shows peaks mainly at BPFO denoted by fod and its harmonic denoted by 2fod. The results have been validated with experimentation under different defect sizes on the outer race. The frequency spectra obtained from experimentation also shows peak at BPFO and its harmonics and also at the shaft frequency and its harmonics.

(2) The model very accurately shows decrease in the amplitude level when the angular position of the defect is kept away from the load zone. It is clear from the model that with the increase in the size of the defect, the vibration amplitude increases. Similarly, for two defects on outer race, vibration amplitude is almost doubled as compared to a single defect on outer race.

(3) There is margin of difference in the amplitude level predicted by the model and obtained through the experimentation. This is because of the fact that the theoretical model cannot account for contribution of each element in the vibration of rotor bearing system.

(4) In this model, the pulse generated by striking the defect is modeled according to the physical phenomenon using the blending functions of the cubic hermite spline. There are very few studies on modeling the defect using splines. The modeling of the defect pulse using cubic Hermite spline is based on the assumption that displacements at the control points (intermediate points) are not known. Instead displacements at the start and end points are known which are -1 and +1 respectively.

(5) This model simulates the defect on outer race only. While simulating the defects on inner race with spline, major changes are required to be done in the mathematical model. This being the first step of using the spline for modelling the defect pulse, the present study is limited to the defect on outer race only. In the next study, efforts will be made to implement the cubic hermite spline for the defective inner race and the defective ball.

Acknowledgment

This work is partly supported by the research grant received from the Board of College and University Development (BCUD), University of Pune, India.

Nomenclature

n_c : Rotational speed of cage (rpm)
n_s : Rotational speed of shaft (rpm)
ω_c : Angular velocity of cage (rad/sec)
ω_r : Angular velocity of ball (rad/sec)
D : Diameter of ball (m)

d_m : Pitch diameter (m)
γ : Radial clearance (μm)
δ_{max} : Maximum deflection in the direction of radial load
ε : Load distribution factor
x,y : Deflection along X and Y direction (m)
n : Load-deflection exponent
K : Load-deflection factor
$\sum\rho$: Curvature sum
F (ρ) : Curvature difference
δ^* : Dimensionless contact deformation
Δ : Additional deflection (m)
C : Damping factor (N s/m)
M : Mass of rotor (kg)
W : Radial load (N)
BPFO : Ball pass frequency outer race (Hz)

References

[1] C. S. Sunnersjo, Varying compliance vibrations of rolling bearings, *Journal of Sound and Vibration*, 58 (3) (1978) 363-373.
[2] T. A. Harris, *Rolling bearing analysis*, Third Ed. John Wiley and Sons, New York, USA (2001).
[3] T. S. Nisbet and G. W. Mullett, *Rolling bearings in service: Interpretation of types of damage*, Hutchinson (1978).
[4] N. Tandon and A. Choudhury, A review of vibration and acoustic measurement methods for the detection of defects in rolling element bearings, *Tribology International*, 32 (1999) 469-480.
[5] P. D. McFadden and J. D. Smith, Model for the vibration produced by a single point defect in a rolling element bearing, *Journal of Sound and Vibration*, 96 (1) (1984) 69-82.
[6] P. D. McFadden and J. D. Smith, Model for the vibration produced by multiple point defects in a rolling element bearing, *Journal of Sound and Vibration*, 98 (2) (1985) 263-73.
[7] Y. T. Su and S. J. Lin, On initial fault detection of a tapered roller bearing: frequency domain analysis, *Journal of Sound and Vibration*, 155 (1) (1992) 75-84.
[8] N. Tandon and A. Choudhury, An analytical model for the prediction of the vibration response of rolling element bearings due to a localized defect, *Journal of Sound and Vibration*, 205 (3) (1997) 275-92.
[9] N. Sawalhi and R. B. Randall, Simulating gear and bearing interactions in presence of faults: Part I. The combined gear bearing dynamic model and the simulation of localized bearing faults, *Mech. Syst. Signal Process*, 22 (2008) 1924-1951.
[10] V. N. Patel, N. Tandon and R. K. Pandey, A dynamic model for vibration studies of deep groove ball bearings considering single and multiple defects in races, *Journal of Tribology*, 132 (2010) 041101-1-10.
[11] M. S. Patil, Jose Mathew, P. K. Rajendrakumar and Sandeep Desai, A theoretical model to predict the effect of localized defect on vibrations associated with ball bearing, *International Journal of Mechanical Sciences*, 52 (2010) 1193-1201.
[12] S. P. Harsha, K. Sandeep1 and R. Prakash, Non-linear dynamic behaviors of rolling element bearings due to surface waviness, *Journal of Sound and Vibration*, 272 (2004) 557-580.
[13] R. K. Purohit and K. Purohit, Dynamic analysis of ball bearings with effect of preload and number of balls Int. *Journal of Applied Mechanics and Engineering*, 11 (1) (2006) 77-91.
[14] Yi Guo and Robert G. Parker, Stiffness matrix calculation of rolling element bearings using a finite element/contact mechanics model, *Mechanism and Machine Theory*, 51 (2012) 32-45.

A. D. Sahasrabudhe did his Bachelor of Engineering Degree in Mechanical Engineering with a Gold Medal from Karnataka University followed by Master of Engineering and Ph.D. from Indian Institute of Science, Bangalore with UGC fellowship.

P. G. Kulkarni is currently a Ph.D. student of COEP, University of Pune, India. He did his Master of Engineering in Mechanical Engineering from Walchand College of Engineering, Sangli. His research interests include condition monitoring and signal analysis.